Rab33A: Characterization, Expression, and Suppression by Epigenetic Modification

Elaine Cheng[1], Sergio E. Trombetta[2], Daniela Kovacs[1,7], Robert D. Beech[3], Stephan Ariyan[4], Miguel Reyes-Mugica[5], Jennifer M. McNiff[1,5], Deepak Narayan[4], Harriet M. Kluger[6], Mauro Picardo[7] and Ruth Halaban[1]

Rab33A, a member of the small GTPase superfamily, is an X-linked gene that is expressed in brain, lymphocytes, and normal melanocytes, but is downregulated in melanoma cells. We demonstrate that in normal melanocytes Rab33A colocalizes with melanosomal proteins and that a constitutively active GTPase mutant suppresses their transport to the melanosomes. In the brain, *Rab33A* is present throughout the cortex, as well as in the hippocampal CA fields. A survey of melanocytic lesions demonstrated that aberrant downregulation of Rab33A is an early event that is already prevalent in melanocytes of giant congenital nevi. Analyses of bisulfite-modified DNA revealed that *Rab33A* is regulated by DNA methylation of a specific promoter region proximal to the transcription initiation site, and that suppression of *Rab33A* in melanoma cells recapitulates normal processes that control silencing of X-linked genes, but not tissue specific gene expression. This information is important for understanding carcinogenesis as well as other aberrant processes because Rab33A may have an important role in disorders involving X-chromosome-linked genes associated with vesicular transport.

Journal of Investigative Dermatology (2006) **126,** 2257–2271. doi:10.1038/sj.jid.5700386; published online 29 June 2006

INTRODUCTION

Genome-wide differential gene expression analyses of normal human melanocytes as compared to cells isolated from advanced melanoma lesions have revealed changes that are likely to influence cellular behavior and be associated with the malignant phenotype (e.g. see Hoek *et al.*, 2004). Our previous work demonstrated that several genes encoding Rab small GTPases were prominently downregulated in melanoma cells compared to normal melanocytes, including Rab27A, Rab31, Rab32, Rab33A, and Rab38 (Hoek *et al.*, 2004). From this group, Rab33A was chosen for further analysis because (a) gene transcripts were uniformly suppressed in the six independent melanoma cell strains tested (Hoek *et al.*, 2004); (b) the gene is expressed in a tissue-specific manner, being high in brain, lymphoid (particularly B lymphoblasts), and monocytic cells and barely detectable in other tissues (Zheng *et al.*, 1997, 1998; Su *et al.*, 2004); and (c) the gene is localized in chromosomal region Xq26.1 and is likely to be subjected to normal X-inactivation processes. Although the function of Rab33A is not known, a recent study supports the notion that it participates in host immune responses because Rab33A is significantly reduced in CD3-positive lymphocytes in patients with tuberculosis compared to healthy individuals (Jacobsen *et al.*, 2005).

Chromosomal modification via DNA methylation is a key mechanism implicated in tissue-specific gene expression, X chromosome inactivation, and the suppression of imprinted genes (Jaenisch and Bird, 2003). Methylation of DNA at the C-5 position of cytosine (5-methyl cytosine) occurs in the majority of adult tissues almost exclusively in CpG dinucleotides (Costello and Plass, 2001; Paulsen and Ferguson-Smith, 2001). This dinucleotide is relatively uncommon in most of the genome (approximately 1 per 50–100 bp, which is one-third to one-sixth the amount expected randomly), but is enriched in short stretches of CpG-dense DNA known as CpG-rich islands that are on average 1–2 kb in length. There are approximately 30,000 such islands in the sequenced portion of the human genome, and roughly half of these islands are thought to overlap promoter regions, because they surround the 5′ ends of genes (Costello and Plass, 2001; Bird, 2002). The presence of methylated cytosines alters the

[1]*Department of Dermatology, Yale University School of Medicine, New Haven, Connecticut, USA;* [2]*Department of Cell Biology, Yale University School of Medicine, New Haven, Connecticut, USA;* [3]*Department of Psychiatry, Yale University School of Medicine, New Haven, Connecticut, USA;* [4]*Department of Surgery, Yale University School of Medicine, New Haven, Connecticut, USA;* [5]*Department of Pathology, Yale University School of Medicine, New Haven, Connecticut, USA;* [6]*Comprehensive Cancer Center Section of Medical Oncology, Yale University School of Medicine, New Haven, Connecticut, USA and* [7]*Istituto Dermatologico San Gallicano, IRCCS, Rome, Italy*

Correspondence: Dr Ruth Halaban, Department of Dermatology, Yale University School of Medicine, HRT 609B, PO Box 208059, 15 York St, HRT 610, New Haven, Connecticut 06520-8059, USA.
E-mail: ruth.halaban@yale.edu

Abbreviations: 5-Aza-CdR, 5-Aza-2′-deoxy-cytidine; BS, bisulfite; COBRA, combined bisulfite restriction analysis; KPBS, potassium-phosphate buffered saline; MSP, methylation-specific PCR; RT-PCR, reverse transcriptase-PCR; TICVA, melanocyte medium containing TPA (12-O-tetradecanoyl phorbol-13-acetate), IBMX (3-isobutyl-1-methyl xanthine), Na_3VO_4 and dbcAMP (N^6,2′-O-dibutyryladenosine 3:5-cyclic monophosphate); wt, wild-type

Received 13 February 2006; revised 6 April 2006; accepted 10 April 2006; published online 29 June 2006

chromatin structure, and in most cases, represses the embedded promoter and consequently inactivates the gene (Klose and Bird, 2006).

Aberrant patterns of DNA methylation are frequent in a variety of cancers including melanoma (Hoon *et al.*, 2004; Feinberg and Tycko, 2004; Esteller, 2005a, b). Many genes associated with tumor suppression, apoptosis, DNA repair, adhesion, and response to interferon are silenced by this process in cancer cells (Esteller *et al.*, 1999, 2001, 2002; Feinberg and Tycko, 2004; Ballestar and Esteller, 2005a, b; Chen and Baylin, 2005). We therefore surmised that CpG methylation of the *Rab33A* promoter might contribute to its downregulation in melanoma cells.

In this report, we investigated Rab33A cell-specific expression and its subcellular localization within melanocytes and tested its function by ectopic expression of dominant-negative and dominant-positive mutant proteins. We then assessed the role of promoter methylation in the modulation of Rab33A transcription. We demonstrate that (a) in melanocytes, Rab33A colocalizes with melanosomal proteins; (b) in mouse brains, it is found in specific regions associated with memory and cognitive functions; (c) ectopic expression of a Rab33A mutant with reduced endogenous GTPase activity attenuated the levels of melanosomal proteins throughout the cell; and (d) downregulation of Rab33A in melanoma cells is orchestrated by methylation of a specific CpG island region that also governs this gene's normal X chromosome silencing, but not tissue-specific suppression.

RESULTS

Tissue-specific expression and subcellular localization of Rab33A

The melanocyte-specific expression of *Rab33A* in skin cells was demonstrated by reverse transcriptase-PCR (RT-PCR) analysis of gene transcripts. *Rab33A* was specifically expressed in melanocytes (M), but not in keratinocytes (K), fibroblasts (F), or endothelial cells (E) (Figure 1a).

To examine endogenous and ectopically expressed proteins, we raised polyclonal antibodies against a peptide corresponding to an N-terminal sequence unique to Rab33A. We also subcloned *Rab33A* from human melanocyte cDNA and constructed a Flag-tagged Rab33A mammalian expression vector. The plasmid was transfected into melanoma cells (501 mel lacking endogenous Rab33A), and the transiently transfected cells were used to ascertain the specificity of the anti-Rab33A polyclonal antibodies, and to determine the subcellular localization of the ectopic protein. Successive Western blotting with anti-Flag mAb and anti-RAB33A peptide antibodies confirmed that each recognized a single band with similar migration pattern, validating the specificity of the Rab33A antibodies and the integrity of the fusion gene construct (Figure 1b). Furthermore, the anti-Rab33A antibodies recognized a single protein band in melanocyte (M) lysates from normal human (h) and mouse (m) skin and in mouse brain extract, all displaying a slightly faster mobility than FlagRab33A, as expected from the additional Flag epitope (eight amino-acid residues) in the construct.

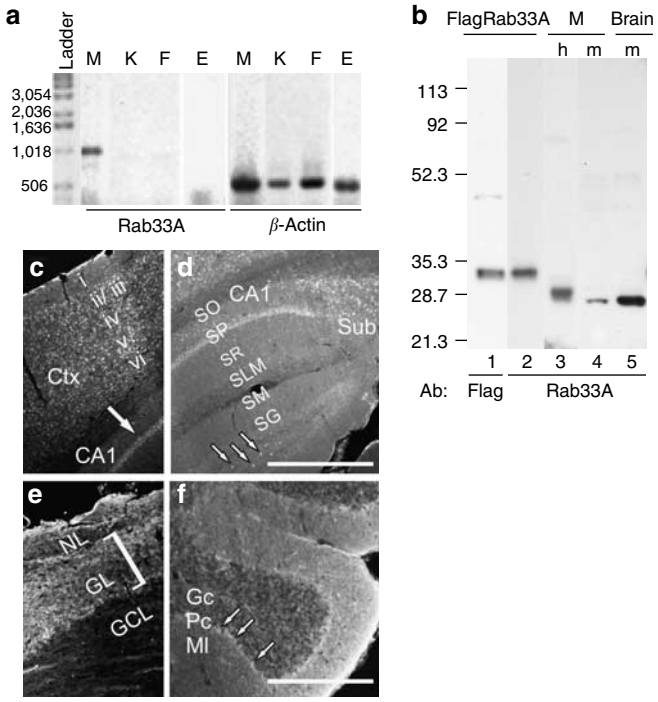

Figure 1. Tissue-specific expression and subcellular localization of Rab33A. (**a**) The figure shows Rab33A gene transcripts in normal human melanocytes (M), keratinocytes (K), fibroblasts (F), and endothelial cells (E) compared to β-actin employing RT-PCR. Rab33A primer pair that amplifies the 835 bp was employed in this RT-PCR analysis (35 cycles). (**b**) Western blot analysis of Rab33A in transfected 501 mel melanoma cells (lanes 1 and 2), normal human melanocytes (lane 3), normal mouse melanocytes (lane 4), and mouse brain (lane 5). The membrane was blotted with anti-Flag mAb (Flag) or with anti-Rab33A antibodies as indicated. (**c–f**) Expression of Rab33A in the adult mouse brain. The figure shows parasagittal sections (35 μm) from adult mouse brain stained with anti-Rab33A peptide antibodies and photographed at original magnification ×20. (**c**) Cortex. Rab33A is expressed throughout all cellular layers of the cortex (ii–vi), as well as in the pyramidal cell layer of the hippocampus below (arrow). (**d**) Hippocampus. Expression is seen in the stratum pyramidale as well as in the adjacent subiculum (Sub) and some isolated cells in the hilus of the dentate gyrus (arrows). SO, stratum oriens; SP, stratum pyramidale; SR, stratum radiatum, SLM, stratum lacunosum moleculare; SM, stratum moleculare; SG, stratum granulare. (**e**) Olfactory bulb. Expression of Rab33A in the olfactory bulb is highest in the glomerular layer (GL, bracket). NL, olfactory nerve layer. GCL, granule cell layer. Panel d scale bar of 500 μm applies to panels c–e. (**f**) Cerebellum. Expression is seen in the pyramidal cell layer (PC, arrows) and in the underlying granule cell layer (Gc). Ml, molecular layer. Bar = 250 μm.

Immunostaining of mouse brain with anti-Rab33A antibodies revealed high levels of expression in the cortex and hippocampus, with lower levels in other brain regions including the olfactory bulb and cerebellum. Rab33A was present in the cortex throughout all cellular layers (Figure 1c, ii–vi). In the hippocampus, expression was seen in the stratum pyramidale as well as in the adjacent subiculum and some isolated cells in the hilus of the dentate gyrus stratum (Figure 1d, regions as marked). Rab33A was also expressed in the glomerular layer of the olfactory bulb (Figure 1e, bracket), and in the pyramidal cell and granule cell layers of the cerebellum (Figure 1f).

Rab33A colocalizes with melanosomal proteins, and its mutant form suppresses transport to the melanosomes

Immunofluorescence microscopy of FlagRab33A-transfected melanoma cells demonstrated that the anti-Flag and anti-Rab33A antibodies labeled the same intracellular compartments in the perinuclear region, dendrites, and dendrite tips, confirming that the Rab33A peptide antibodies recognized Rab33A (Figure 2a). The endogenous Rab33A in normal melanocytes was distributed in a similar vesicular pattern that was also shared by the melanosomal protein Tyrp1 (Vijayasaradhi *et al.*, 1995; Halaban *et al.*, 2000; Halaban *et al.*, 2001) and gp100 (Figure 2b and c, yellow

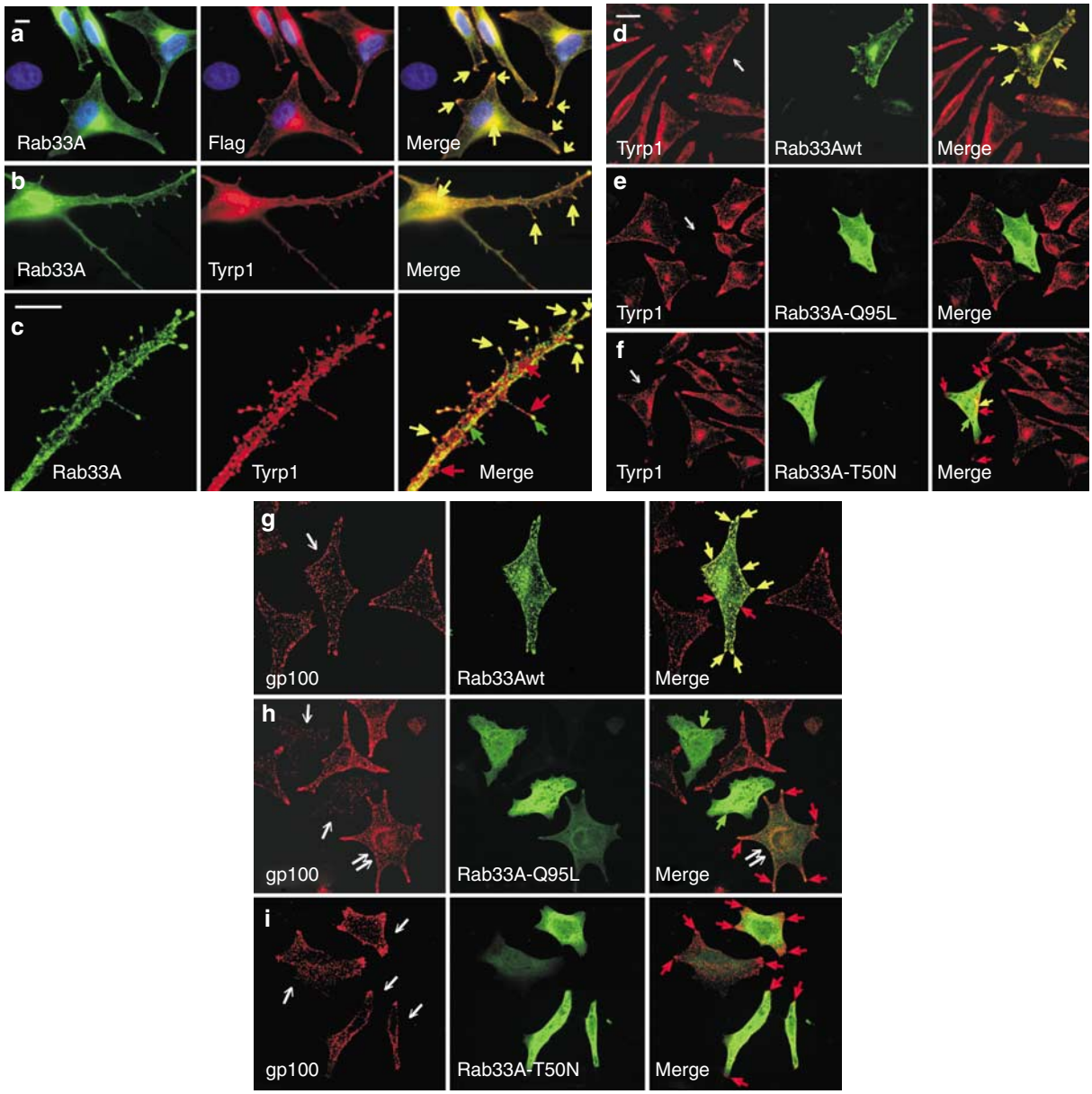

Figure 2. Subcellular localization of Rab33A, Tyrp1, and gp100 in melanocytic cells. (**a–c**) Rab33A is localized in vesicular compartments. (**a**) Immunofluorescence of FlagRab33A-transfected melanoma cells probed with anti-Rab33A (green), anti-Flag mAb (red), and the merged images (Merge). Cells were fixed 2 days after transfection. The DAPI-positive cell devoid of any staining (left side of images) represents a cell that is not expressing FlagRab33A and is also negative for endogenous Rab33A as expected from gene expression analysis and Western blotting. The 10 μm scale bar is for panels a and b. Panels b and c are immunofluorescence images of normal human melanocytes stained with anti-Rab33A (green), or anti-Tyrp1 mAb TA99 (red) and the merged images (Merge). The enlarged image of a dendrite in panel c taken by confocal microscopy shows vesicles in which Rab33A colocalizes with Tyrp1 (yellow arrows), and vesicles in which the two do not share the same compartment (red and green arrows). Bar = 10 μm. (**d–i**) Subcellular localization of wt and mutant FlagRab33A proteins compared to Tyrp1 and gp100 in transiently (1 day) transfected 501 mel melanoma cells. (**d–f**) Immunostaining of Tyrp1 (TA99 mAb, red), Rab33A (anti-peptide polyclonal antibodies, green), and merged image (Merge). Cells were transfected with wt Rab33A (Rab33Awt), mutant Rab33A-Q95L, or mutant Rab33A-T50N as indicated. (**g–i**) Immunostaining of gp100 (HMB45 mAb, red), Rab33A (green), and merged images (Merge). The white arrows in panels d–i point at Rab33A-Q95L- and Rab33A-T50N-expressing cells. In the merged images, yellow arrows indicate colocalized proteins, whereas green and red arrows point at sites in which Rab33A and melanosomal proteins, respectively, are not in the same compartment. The 10 μm bar in panel d is for all panels in d–i.

arrows), although the colocalization was not complete (Figure 2c, red and green arrows).

The effect of Rab33A on Tyrp1 and gp100 was tested by ectopic expression of gain- and loss-of-function Rab33A mutants. Constitutively active Rab33A was generated by the substitution of Gln95 by Leu in FlagRab33A (Rab33A-Q95L), a mutation in the second motif of the GTP-binding domain that is expected to decrease GTPase activity as shown for other Rab proteins (Feig, 1999). On the other hand, inactive Rab33A was constructed by the substitution of Thr50 by Asn in FlagRab33A (Rab33A-T50N). This mutation in the first motif of Rab33A GTP-binding domain is expected to block the GDP-to-GTP exchange necessary for Rab activation (Feig, 1999). Immunofluorescence analyses of transiently transfected cells revealed that the mutant Rab33A proteins were distributed throughout the cytoplasm and no longer colocalized with Tyrp1 or gp100 (Figure 2, green fluorescent cells in panels e and f compared to panel d, and panels h and i compared to panel g). Furthermore, the levels of Tyrp1 and gp100 were dramatically decreased in cells expressing high levels of Rab33A-Q95L relative to untransfected neighboring cells and wild-type (wt) Rab33A transfectants (Figure 2a and h, red fluorescent cells marked with white arrows). This effect was less distinctive in cells expressing low levels of Rab33A-Q95L (Figure 2h, cell marked with double white arrow). In contrast, the inactive mutant Rab33A-T50N did not significantly disturb the distribution and levels of Tyrp1 and gp100 (Figure 2f and i). These latter results are consistent with the observation that Tyrp1 and gp100 are normally localized to melanosomes in cells devoid of Rab33A (such as the 501 mel cells used for transfection).

Early suppression of Rab33A in melanocytic lesions

As mentioned above, we first discovered the loss of *Rab33A* mRNA expression in melanoma cells as compared to normal melanocytes by using the Affymetrix expression analysis approach (Hoek *et al.*, 2004). We now examine Rab33A protein levels by Western blot analysis employing melanocytes from benign lesions, short-term cultured melanoma cells, established melanoma cell strains, and snap-frozen tumors. The results show that suppression of Rab33A is an early event in melanocytic lesions. The protein was present in nevocytes from small nevi (three independent donors) but not in six out of seven nevocytes from congenital giant nevi (Figure 3a, compare lanes 3–5 to lanes 6–12). This pattern of expression/suppression was not related to age or gender, and suppression was specific to the lesional nevocytes. The levels of Rab33A were normal in melanocytes from uninvolved skin of the same patient with giant nevus (Figure 3a, YUYAG, compare lanes 12 and 13). There was also no relationship between age and Rab33A suppression. The YUZUV, YUBUR, YUGIR, YUWAC, YUWAL, and YUYAG non-expressing nevocytes originated from individuals who were 2.5 years, 11 months, 3, 4, 1, and 34 years old, respectively (lanes 6, 7, 8, 9, 10, and 12), whereas the expressing YUFUR, YUHOB, YUPAR, and YUOLD nevocytes were from patients 13, 29, 25, and 10 years old, respectively (lanes 3, 4, and 5). Although all the samples deficient in Rab33A were from

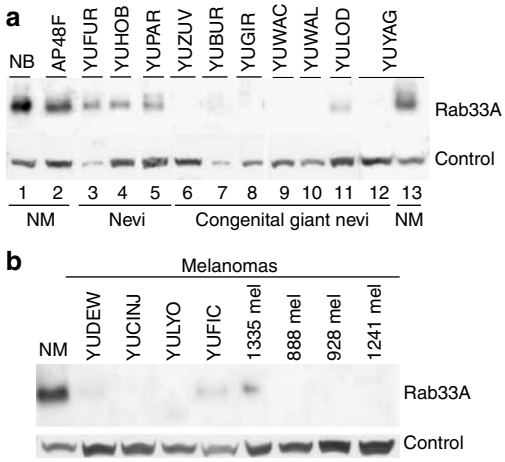

Figure 3. Downregulation of Rab33A in giant congenital nevi and melanomas. (**a**) Western blot analysis of Rab33A employing cell extracts from normal melanocytes (NM) isolated from foreskins (NB) and adult female skin AP48F (lanes 1 and 2, respectively), small nevi (lanes 3–5), congenital giant nevi (lanes 6–12), and the normal skin of YUYAG adjacent to the giant nevus (lane 13). (**b**) Western blot analysis of Rab33A in several metastatic melanomas (as indicated) compared to normal melanocytes (NM) from adult skin AP48F. Actin was used as control for protein loading.

female donors, there were equal numbers of male and female donors among the expressing group (compare samples from male donors in lanes 3 and, 11 to samples from female donors in lanes 4 and 5), suggesting that gender did not play a role in Rab33A expression. In addition, culture conditions did not affect expression because all nevocyte samples were grown in the same medium and tested after one or two passages in culture. Moreover, one-day incubations of melanoma cells (1335 mel) in melanocyte medium (TICVA – medium containing TPA (12-*O*-tetradecanoyl phorbol-13-acetate), IBMX (3-isobutyl-1-methyl xanthine), Na_3VO_4, and dbcAMP (N^6,2′-*O*-dibutyryladenosine 3:5-cyclic monophosphate)), or normal melanocytes in melanoma medium did not change Rab33A mRNA levels in the respective cells (data not shown).

Rab33A was uniformly downregulated in melanoma cells and melanoma tumors, confirming our original results based on mRNA levels (Hoek *et al.*, 2004). Very faint reactive bands were detected in only three out of 15 melanoma cell strains and tissue samples tested (Figure 3b, YUDEW, YUFIC, and 1335 mel; data not shown). These observations could not be expanded to a much larger sample size because attempts to probe melanoma tissue microarrays with the anti-Rab33A peptide antibodies failed owing to excessive nonspecific background.

Rab33A promoter methylation

Four CpG-rich islands are present in the Rab33A proximal promoter and exon 1 (identified by the web-based MethPrime program; Figure 4a). The methylation of three of these CpG islands flanking the initiation start site was assessed by (combined bisulfite restriction analysis) COBRA, BS-MSP (bisulfite methylation-specific PCR), and BS sequencing

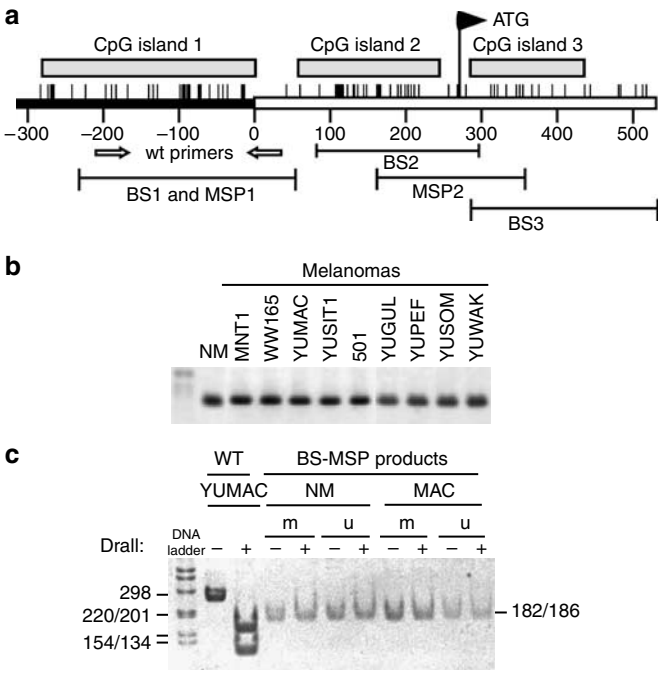

Figure 4. Rab33A promoter is intact and undergoes complete BS modification. (**a**) Schematic representation of Rab33A promoter region and first exon. The genomic structure of Rab33A is based on Rab33A mRNA sequence (Accession no. NM_004794) and human DNA sequence from clone RP3-438D16 on chromosome Xq24-26.1, accession number AL139234. The horizontal line indicates the promoter region and the first exon (box). The vertical arrow marks the ATG open reading frame site of Rab33A, the multiple short bars above the line are sites of CpG dinucleotides, and gray boxes CpG islands 1–3 (identified by the MethPrime program). The scale below the line represents bp. The arrows indicate the amplification sites of Rab33A unmodified (wt) DNA. The bracketed bars delineate the regions amplified with BS primers and analyzed for DNA methylation. All primers are listed in Table 2. (**b**) Rab33A promoter is intact in melanoma cells. Unmodified Rab33A promoter from normal melanocytes (NM), cultured melanoma cell strains MNT1, WW165, YUMAC, YUSIT1, and 501 mel, and melanoma tumors YUGUL, YUPEF, YUSOM, and YUWAK (see Table 1 for more details) was amplified by employing Rab33A wt primers (Table 2). Reaction products were separated in agarose gel and visualized under UV light. (**c**) Validation of BS modification. Non-converted DNA from the YUMAC melanoma was amplified with wt primers (Rab33Awt), and BS-converted DNA samples from normal melanocytes (NM) and YUMAC melanoma cells were amplified first with BS1 primer pairs that bind modified DNA in a non-CpG region. A portion of the amplified and purified 263 bp fragments (1/20th) was then subjected to a second round of amplification (35 cycles) with nested MSP primers that recognize either methylated (m) or unmethylated (u) DNA (Table 2, M1 and U1 primers), generating products of 182 and 186 bp, respectively (BS-MSP). Half of the reaction products were kept as control (–), whereas the other half were digested with *Dra*II restriction enzyme (+) that cuts the sequence GG/GTCCT in a non-CpG dinucleotide segment. Products were separated in 1% agarose gel and visualized under UVB light. The results show that *Dra*II digested the 265-bp wt DNA to two fragments of 155 and 110 bp but not the methylated and unmethylated 182 and 186 bp fragments, respectively, which were otherwise expected to generate 124 and 53 bp fragments, indicating complete conversion by BS.

(Herman *et al.*, 1996; Sasaki *et al.*, 2003) as illustrated in Figure 4a. These procedures take advantage of DNA sequence differences between methylated and unmethylated alleles after BS DNA modification, which deaminates unmethylated cytosine converting it to uracil, but spares methylated cytosine (Frommer *et al.*, 1992). Therefore, after PCR amplification, unmethylated DNA molecules will have an A:T pair instead of C:G, whereas the methylated (5-methylcytosine) pairs are resistant to this modification and remain as cytosine (C:G). In COBRA analyses, we used restriction enzymes such as *Hha*I, *Taq*$^{\alpha}$I, *Bsi*EI, *Nco*I, or *Mae*II that cut unconverted (methylated) but not converted (unmethylated) DNA to assess methylation.

We first verified that *Rab33A* is intact in several melanoma cell strains and tumor samples by amplifying the unmodified promoter region with wt primers (Figure 4b). In addition, we confirmed that the DNA was completely modified by the BS treatment by demonstrating that amplified wt non-converted but not BS converted DNA was digested by *Dra*II, a restriction enzyme that targets GG/GTCCT sites (Figure 4c). The methylation status of the BS converted DNA was also confirmed by digesting the gel purified MSP fragments with *Nco*I. This enzyme digests the non-CpG segment C/CATTGG in the unconverted DNA generating 133 and 72 bp fragments, whereas the converted (TTATGG) DNA remains intact. There were no fragments after digestion of several samples from melanoma cells, indicating complete BS conversion of DNA (data not shown). The methylation analyses described below showed that, among the three CpG islands, CpG island 2 was critical for Rab33A expression.

Analysis of CpG islands 1 and 3. COBRA analysis ruled out methylation of CpG1 and CpG3 as the basis for suppression of gene expression. The X-inactive chromosome was not methylated in this region because CpG1 was resistant to *Hha*I digestion regardless of gender (Figure 5a, compare NM lanes 1 and 2). In addition, this region was not methylated in expressing YUOLD nevocytes and non-expressing YUDEW melanoma cells (resistant to *Hha*I digestion). CpG1 was completely methylated only in the YUMAC melanoma cell strain (Figure 5a, and confirmed by BS sequencing, Figure S1). Age did not play a role in the methylation pattern because the two non-expressing melanoma cell strains YUDEW and YUMAC originated from 68-year-old patients (Table 1).

Methylation analysis of fresh newborn skin, and formalin-fixed paraffin-embedded nevi and melanoma lesions, all derived from male individuals, showed again that CpG1 methylation did not correlate with the malignant state. *Taq*$^{\alpha}$I and *Hha*I digestion products were present in the two small nevi YDP96 and YDP44, and two of the three melanoma lesions analyzed (Figure 5b, compare YDP05 and YDP50 to YDP60).

The region analyzed in CpG3 (Figure 6a) was composed of methylated and unmethylated alleles regardless of gender or Rab33A expression (Figure 6b, compare expressing AP48F normal melanocytes to non-expressing YUDEW melanoma cells). The mixture of alleles indicates variations within the cell population. BS sequencing also showed that CpG3 was highly methylated in normal melanocytes, nevocytes (YUOLD and YUYAG), snap-frozen melanoma tumor (YUPEF), and WW165 primary melanoma cells. Low levels of

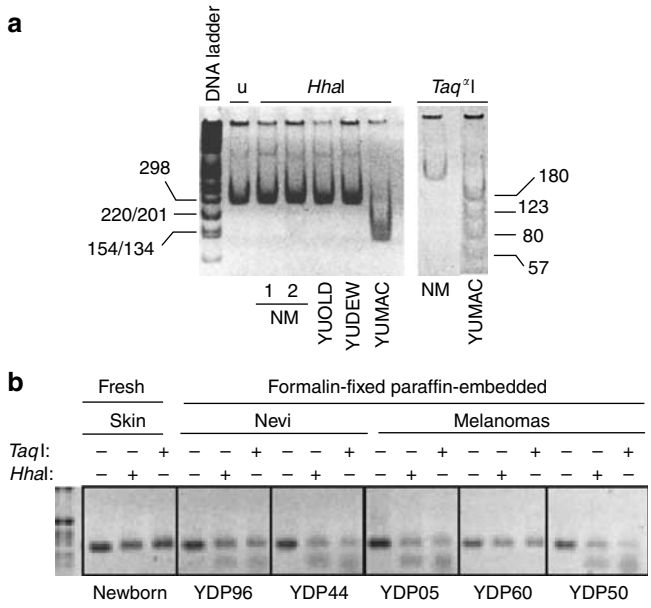

Figure 5. COBRA analysis of CpG island 1 (CpG1). (**a**) Purified DNA samples from foreskin (male) and adult AP48F (female) melanocytes (NM; lanes 1 and 2, respectively), giant nevus melanocytes (YUOLD), and melanoma cells (YUDEW and YUMAC) were treated with BS and the 263 bp region of Rab33A CpG1 was PCR amplified with BS1 primer pairs (Table 2), purified and digested with *Hha*I or *Taq*$^{\alpha}$I. Digestion products were separated in 8% polyacrylamide gel and visualized under UVB light. U, uncut fragment. The sizes (bp) of 1 kb DNA ladder markers are indicated on the left-hand side, and digestion products on the right-hand side. In this polyacrylamide gel and all subsequent gels, DNA fragments under analysis display slower migration pattern than expected owing to the presence of BSA in the reaction mixture. (**b**) BS-treated DNA from normal human melanocytes (NM), newborn skin (Skin), formalin-fixed and paraffin-embedded nevi (YDP96 and YDP44), and primary melanoma lesions (YDP05, YDP 60, YDP50) were processed and digested with *Taq*$^{\alpha}$I or *Hha*I restriction enzymes (lanes marked with +) as in **a**, except that reaction products were separated in 1% agarose gel.

unmethylated alleles (TG instead of CG) were also detected at equal levels in expressing and non-expressing cells (Figure 6c, compare YUOLD expressing to YUYAG non-expressing nevocytes). Although this region was completely methylated in WW165 melanoma cells, low levels of the unmethylated allele were present in YUPEF tumor almost to the same extent as in nevus cells (YUOLD and YUYAG) (Figure 6c), suggesting that modification of CpG3 is not involved in malignant progression.

CpG islands 2. COBRA, BS-MSP, and BS-sequencing analyses suggested that methylation of CpG2 silences Rab33A expression on the inactive X chromosome and on the functional X chromosome in non-expressing melanoma cells.

COBRA analysis showed that this region (Figure 7a) displayed different methylation patterns between male and female donors. Only the unmethylated allele was detected in foreskin melanocyte because the amplified fragment from BS-modified DNA was resistant to digestion by *Taq*$^{\alpha}$I restriction enzyme. In contrast, the unmethylated and methylated alleles were present in melanocytes from a female donor because *Taq*$^{\alpha}$I-resistant and -sensitive fragments were present (Figure 7b, NM and YUMURJ). The predominant presence of the unmethylated CpG2 allele in expressing melanocytes was further confirmed by BS-MSP analysis (Figure 7d, NM), and BS sequencing (Figure 8, YUOLD, gray boxes).

Inactivation of Rab33A in lesional melanocytes was associated with CpG2 methylation on the functional X chromosome. All amplified BS-modified DNA samples from primary and metastatic melanoma lesions were completely digested by *Taq*$^{\alpha}$I to the expected size fragments of 113 bp (Figure 7b). COBRA analysis with *Hha*I and *Mae*II restriction enzymes provided further evidence that additional CpG dinucleotide pairs were methylated (sensitive) in YUMAC melanoma, but unmethylated (resistant) in normal melanocytes (Figure 7c). Furthermore, BS-MSP analysis showed high levels of methylated CpG2 alleles in the non-expressing congenital giant nevocytes YUZUV and YUBUR, as well as the early primary melanomas WW157, WW88, WW94, and a recurrent melanoma YUCOR (Figure 7d), and predominantly the methylated CpG2 allele in advanced melanomas derived from cultured cells and snap-frozen specimens (Figure 7e and f, respectively). Finally, BS sequencing showed that the methylated allele was predominant in primary melanoma WW165, and metastatic melanoma YUGUL and YUMAC cells (Figure 8, black boxes). These differences in the pattern of methylation did not reflect the age or gender of the donors, because the nevi were from infants and there were equal representations of male and female donors (Table 1).

CpG2 methylation analysis of DNA from freshly excised newborn foreskins shows a predominance of methylated over unmethylated Rab33A CpG2 forms (Figure 7e, skin). Although this pattern can be expected in a tissue in which the melanocytes are in the minority, as will be seen later (Figure 10), CpG2 is also not methylated in undifferentiated cultured keratinocytes.

Taken together, these data indicate that DNA methylation in CpG2, a region located +98 to +141 base pairs downstream of the transcription initiation site, is an aberrant early event in the melanocytic cellular system, occurring in giant nevi that do not express Rab33A and persisting in primary and metastatic melanoma cells and tumors.

Restoration of Rab33A gene expression

Some genes silenced by chromatin modification can be reactivated by the demethylating agent 5-Aza-2′-deoxycytidine (5-Aza-CdR) (see e.g. Hoon *et al.*, 2004). We therefore explored the effect of 5-Aza-CdR on Rab33A expression and promoter demethylation in melanoma cells. Figure 9 shows that short-term exposure (2 days) to low concentrations of the drug (0.1 μM) was effective in restoring Rab33A mRNA expression (Figure 9a) and the demethylated state of some cytosine residues of the Rab33A promoter (Figure 9b, arrows).

Cell-specific Rab33A suppression is not determined by promoter methylation

The results so far suggest that inactivation of Rab33A in melanocytic lesions recapitulated X-chromosomal-silencing process. We therefore further explored whether cell-type-

Table 1. Melanocytic lesions and short-term cultured cells

Specimen	Gender/age (years)	Lesion
(a) Nevus cells in culture		
YUFUR	M/13	Intradermal nevus 0.8 × 0.5 cm
YUPAR	F/25	Intradermal nevus 0.5 × 0.5 cm
YUHOB	F/29	Congenital nevus 4.5 × 3.8 cm
YUBUR	F/1	Giant congenital nevus
YUWAL	F/1	Giant congenital nevus
YUZUV	F/2.5	Giant congenital nevus
YUGIR	F/3	Giant congenital nevus, neurocutaneous melanosis
YUWAC	F/4	Giant congenital nevus
YUOLD	M/10	Giant congenital nevus
YUYAG	M/34	Giant congenital nevus
(b) Snap-frozen nevus		
YUMURJ	F/17	Blue nevus
(c) Formalin-fixed paraffin-embedded nevi		
YDP96	M/60	Intradermal melanocytic nevus (1.2 × 1.0 × 0.6 cm)
YDP44	M50	Intradermal melanocytic nevus (1.3 × 0.9 × 0.5 cm)
(d) Primary melanoma cells		
WW165	F/62	Primary melanoma (2.25 mm)
WW157	M/86	Melanoma *in situ*
WW88	F/71	Superficial spreading invasive melanoma (0.2 mm)
WW94	M/43	Primary melanoma (1.45 mm)
(e) Formalin-fixed paraffin-embedded primary melanomas		
YDP72	M/49	Nodular melanoma (19.0 mm)
YDP05	M/70	Superficial spreading melanoma (4.6 mm)
YDP60	M/28	Superficial spreading melanoma (4.5 mm)
YDP50	M/49	Nodular melanoma (8.7 mm)
(f) Advanced melanoma cells		
YUDAN	F/44	Lymph node metastasis
YUGEN8	F/44	Brain metastasis
YUCOR	F/30	Recurrent melanoma adjacent to the primary lesion
MNT1	M/60	Lymph node metastasis
YUMAC	M/68	Soft tissue metastasis
YUDEW	F/68	Distant metastasis
YUCINJ	F/20	Distant metastasis
YUFIC	M/68	Lymph node metastasis
YULYU	M/71	Distant metastasis
1335 mel	M/47	Lymph node metastasis
YUSIT1	M/67	Metastatic melanoma
(g) Snap-frozen advanced melanoma tumors		
YUGUL	M/57	Lymph node metastasis
YUPEF	M/61	Soft tissue metastasis
YUSOM	M/58	Massive recurrent metastasis
YUWAK	M/56	Local skin metastasis

M, male; F, female.

specific expression in cultured skin cells is also controlled by CpG promoter methylation. COBRA and BS-sequencing analyses revealed that the unmethylated CpG1 and CpG2 alleles were predominant in keratinocytes and fibroblasts isolated from newborn foreskins in a manner similar to normal melanocytes (Figure 10). These results demonstrated that cell-specific expression is controlled by processes that do not include methylation of Rab33A promoter.

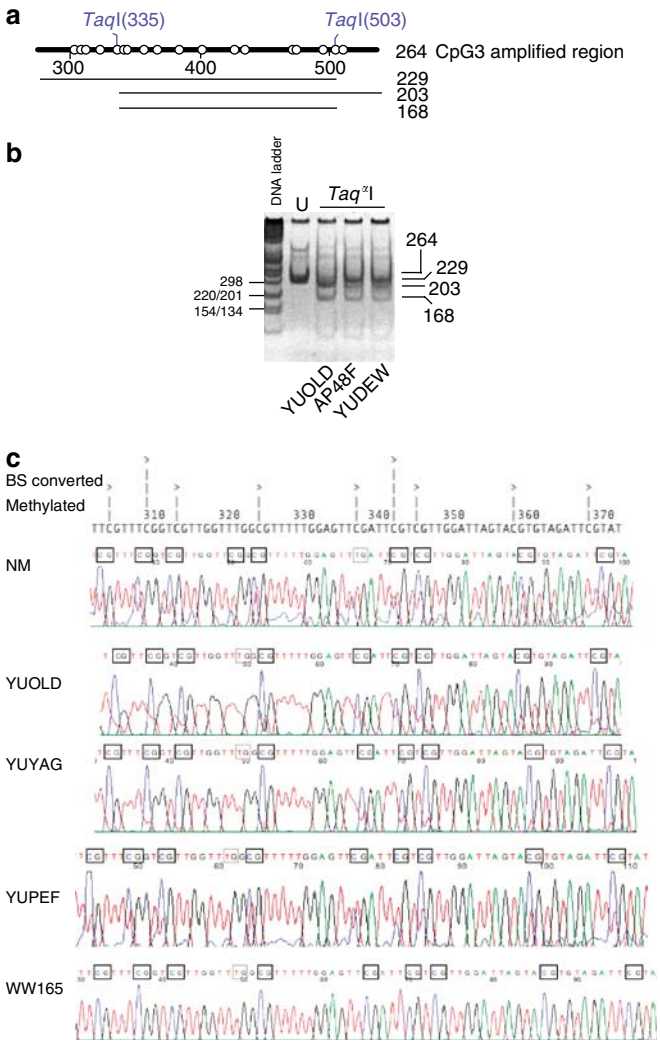

Figure 6. Methylation analysis of Rab33A CpG island 3 (CpG3). (**a**) Schematic representation of CpG3 264 bp amplified region, *Taq*$^{\alpha}$I restriction sites, and locations of CpG pairs (empty circles). (**b**) COBRA analysis of CpG3 in melanocytes from giant nevus (YUOLD), normal adult melanocytes (AP48F), and YUDEW melanoma cells. The BS-modified DNA was amplified with primers that bind in non-CpG dinucleotides regions (BS3, Table 2) generating 264-bp fragments. Other details are as in the legend to Figure 5a. (**c**) BS sequencing results showing that the amplified CpG3 region from Rab33A is mostly methylated in expressing normal melanocytes (NM) and nevocytes (YUOLD), non-expressing YUYAG nevocytes, and YUPEF and WW165 melanoma cells. Methylated CG pairs are marked with black and unmethylated with grey boxes.

DISCUSSION

This report demonstrates that Rab33A was present in melanocytes in vesicles occupied by melanosomal proteins critical for pigmentation. The normal distribution of Tyrp1 and gp100 in Rab33A-null melanoma cells, the normal pigmentation of nevus cells lacking Rab33A (e.g. YUZUV and YUYAG), and the lack of significant effect on these proteins in response to overexpression of the inactive mutant Rab33A-T50N, indicate that Rab33A is not necessary for the transport of melanosomal proteins to the melanosomes. On the other hand, the constitutively active mutant Rab33A-Q95L suppressed the levels of Tyrp1 and gp100 in a dose-dependent manner, suggesting interference with intracellular vesicular transport. The GTP-bound forms of Rab proteins display high affinity for other proteins, such as tethering factors, which in turn complex with SNARE proteins (reviewed by Novick and Zerial, 1997; Deneka *et al.*, 2003). We surmise that Rab33A-Q95L, which was mislocalized in the cytosol, may trap essential ''effectors'', depleting their supply in the vesicular system for other Rab proteins and impairing critical steps required for the transport of Tyrp1 and gp100 to the melanosomes.

It is estimated that the human genome contains at least 60 Rab family members (Stenmark and Olkkonen, 2001). Among those affecting normal pigmentation are Rab27A and Rab38 (reviewed by Seabra and Coudrier, 2004). Mutations in Rab27A impede the transport of subcellular organelles to the periphery, including melanosomes as well as cytotoxic granule transport, causing depigmentation, immune deficiency, and blood disorders. Rab27A mutation is associated with Griscelli syndrome type 2, characterized by partial albinism and uncontrolled T-lymphocyte and macrophage activation (reviewed by Seabra and Coudrier, 2004). On the other hand, abnormality in Rab38 is implicated in the pathogenesis of Hermansky–Pudlak syndrome, an autosomal recessive disorder characterized by albinism and prolonged bleeding (reviewed by Di Pietro and Dell'Angelica, 2005). Rab38 is an endoplasmic reticulum resident protein, and is likely to be responsible to the transport of melanosomal proteins to the Golgi compartment (Osanai *et al.*, 2005). We therefore hypothesize that Rab33A-Q95L disables Rab38 by depriving it from effector proteins. Consequently, the melanosomal proteins are detained in the endoplasmic reticulum and undergo degradation as has been reported for tyrosinase (Halaban *et al.*, 2000, 2001, 2002).

Probing mouse brain sections with Rab33A-specific antibodies indicated expression in the cortex as well as in the hippocampus, regions associated with memory and cognitive functions. The activity of small GTPases of the Rho family is critical for proper brain function because mutations in several genes whose protein products affect this pathway, GDI1 (GDP dissociation inhibitor 1), PHN1 (Oligophrenin-1), PAK3 (p21 (CDKN1A)-activated kinase 3), and ARHGEF6 (Rac/Cdc42 guanine nucleotide exchange factor 6), have already been implicated in X-linked forms of mental retardation (D'Adamo *et al.*, 1998; Berrettini, 2000; Kutsche *et al.*, 2000; Raymond, 2005). In rodents, mutation in Rab23, a negative regulator of the hedgehog signaling pathway, leads to the mouse open brain phenotype (Evans *et al.*, 2005). Rab23 is highly homologous to human Rab33A (Guo *et al.*, 2006). It is thus tempting to speculate that mutations in Rab33A may also be involved in yet unidentified X-linked disorders (particularly Xq26–q27) associated with vesicular trafficking in neurons.

In this report, we also show that silencing *Rab33A* was an early event in the transition from benign to abnormal growth because Rab33A was expressed in melanocytes from normal skin and small nevi, but not in those derived from congenital giant nevi (six out of seven specimen), lesions with

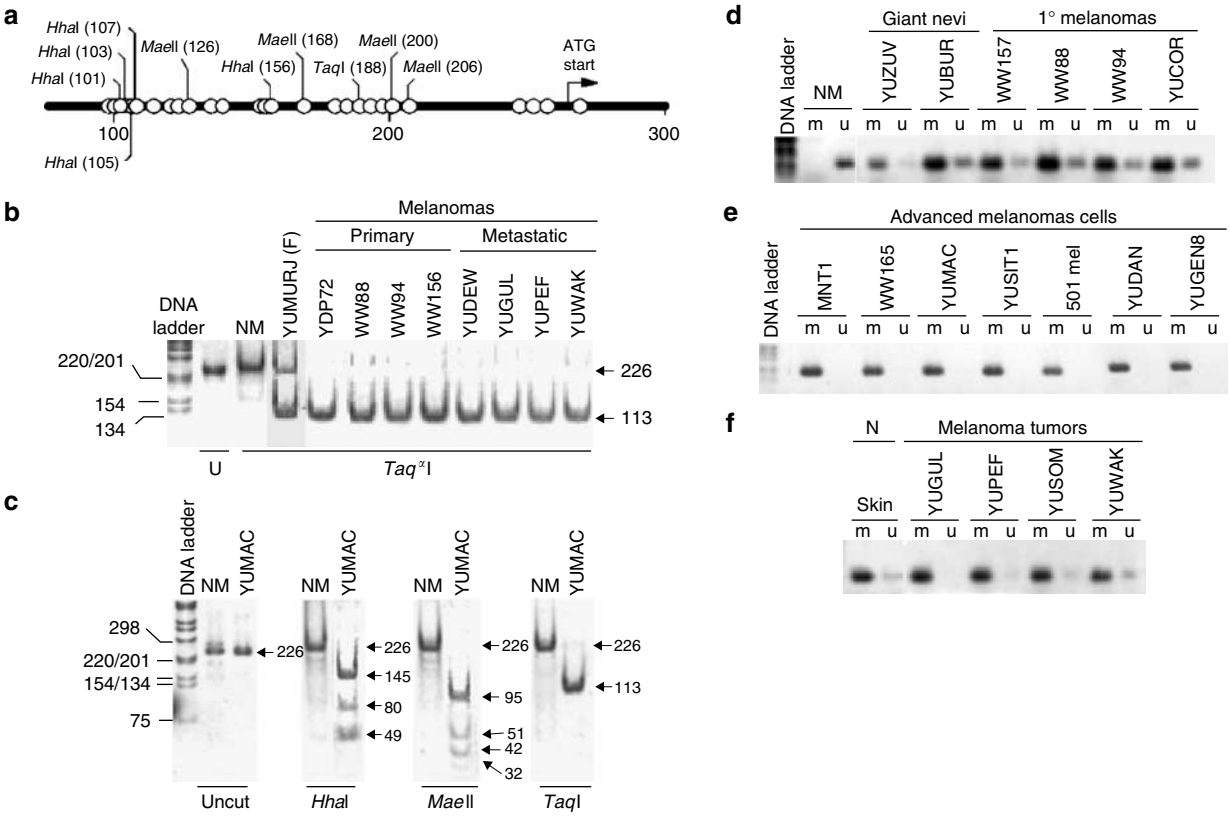

Figure 7. Methylation analysis of Rab33A CpG island 2 (CpG2). (**a**) Schematic representation of CpG2 226 bp amplified region. The *Hha*I, *Taq*$^{\alpha}$I, and *Mae*II restriction sites, ATG translation initiation site (arrow), and locations of CpG pairs (empty circles) are indicated. Numbers on the bottom indicate base pairs from the transcription imitation site (**b–c**) COBRA analysis of CpG2. (**b**) The BS-modified DNA was amplified with primers that bind in non-CpG dinucleotides regions (BS2, Table 2) generating 226-bp fragments. *Taq*$^{\alpha}$I-digested and -undigested (U) DNA samples were separated in 8% polyacrylamide gels followed by visualization under UVB. DNA samples were from normal foreskin melanocytes (NM), snap-frozen blue nevus (YUMURJ) from a female donor (F), formalin-fixed paraffin-embedded primary melanoma (YDP72), primary melanoma (WW88, WW94, WW165), and metastatic melanoma (YUDEW, YUGUL, YUMAC) cells (see also Table 1). (**c**) CpG2 methylation analysis of normal melanocytes (NM) and melanoma (YUMAC) employing *Hha*I, *Mae*II, and *Taq*$^{\alpha}$I restriction enzymes. Digested and undigested (Uncut) DNA samples were separated in 8% polyacrylamide gels followed by visualization under UVB. DNA fragment sizes are indicated by the arrows on the right-hand side. (**d–f**) CpG2 BS-MSP analysis. DNA was isolated from normal human melanocytes (NM), nevus cells, and primary melanoma cells (**d**), cultured metastatic melanoma cell strains (**e**), normal foreskin (N, skin), and snap-frozen melanoma tumors (**f**), as indicated (and listed in Table 1). The BS-modified DNA was PCR amplified with primers that bind to methylated (m) or unmethylated (u) DNA (MSP2, Table 2). Reaction products were separated in 1% agarose gel and visualized under UVB light.

abnormally increased proliferative potential. Furthermore, suppression of Rab33A was prevalent in melanoma cells isolated from primary and advanced lesions. Only extremely low levels of protein were detected in three out of 15 cell strains or freshly excised snap-frozen tumors. Therefore, Rab33A may have other functions that can affect cell proliferation. Overexpression of selected Rab GTPases has been tightly correlated with the pathogenesis of different diseases including cancer (reviewed by Stein *et al.*, 2003). For example, overactivity of Rab25 GTPase enhances the aggressiveness of ovarian and breast cancers (Cheng *et al.*, 2004, 2005).

We identified CpG2, located +98 to +141 bp downstream of the transcription initiation site, as the region critical for Rab33A expression. CpG2 was methylated in the silenced X chromosome, suggesting involvement in X-inactivation processes. Among the giant nevi, CpG2 was highly methylated also on the functional X chromosome in the non-expressing YUZUV and YUBUR, but remained unmethylated in the expressing YUOLD melanocytes, supporting our notion that this epigenetic modification is associated with early aberrant growth processes. CpG2 was also highly methylated in one primary melanoma dissected from a paraffin-embedded block (YDP72), five short-term cultures of primary melanomas (WW88, WW94, WW157, YUCOR), an established primary melanoma cell strain from an advanced lesion (WW165), six strains of metastatic melanomas (YUMAC, MNT1, YUSIT1, 501 mel, YUDAN, and YUGEN8), and four snap-frozen melanoma tumors (YUGUL, YUPEF, YUSOM, and YUWAK). Restoration of Rab33A expression in response to low concentrations of the demethylation drug 5-Aza-CdR provided the evidence that this epigenetic modification is an important process in *Rab33A* suppression. The results showed that Rab33A methylation and gene silencing were common in melanocytic lesions, and may be a useful marker for early transition to an aberrant mode of growth.

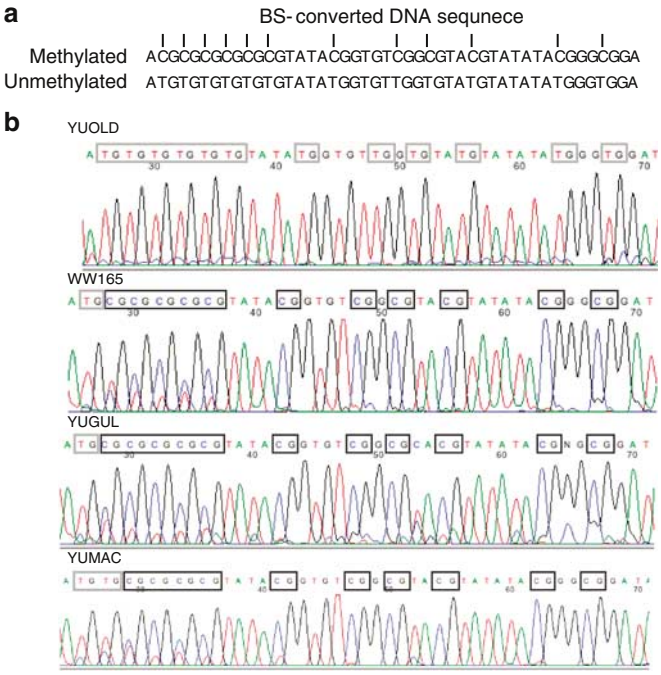

Figure 8. BS sequence analysis of CpG2. (**a**) Predicted sequences of CpG2-methylated and -unmethylated alleles of BS-modified DNA after PCR amplification. Vertical lines mark CG pairs. (**b**) Sequencing results showing that the amplified CpG2 region from Rab33A expressing nevocytes (YUOLD) is unmethylated (gray boxes), whereas those from the regions in non-expressing cells (WW165, YUGUL, and YUMAC) are methylated (black boxes).

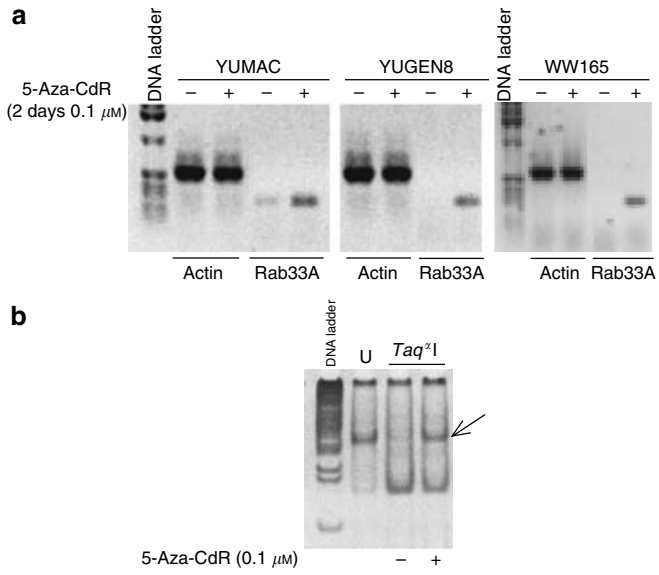

Figure 9. Re-expression of Rab33A in response to demethylation by 5-Aza-CdR. Melanoma cells (YUMAC, YUGEN8, and WW165) were untreated (–) or treated (+) with 5-Aza-CdR (0.1 μM) for 2 days, released into regular medium for an additional 2 days, and then harvested for gene expression and DNA methylation analysis. (**a**) Re-expression of Rab33A mRNA in response to 5-Aza-CdR employing actin as a control. (**b**) Partial restoration of CpG2 demethylated state in YUGEN8 melanoma cells as revealed by the appearance of band resistance to *Taq*$^{\alpha}$I digestion (arrow).

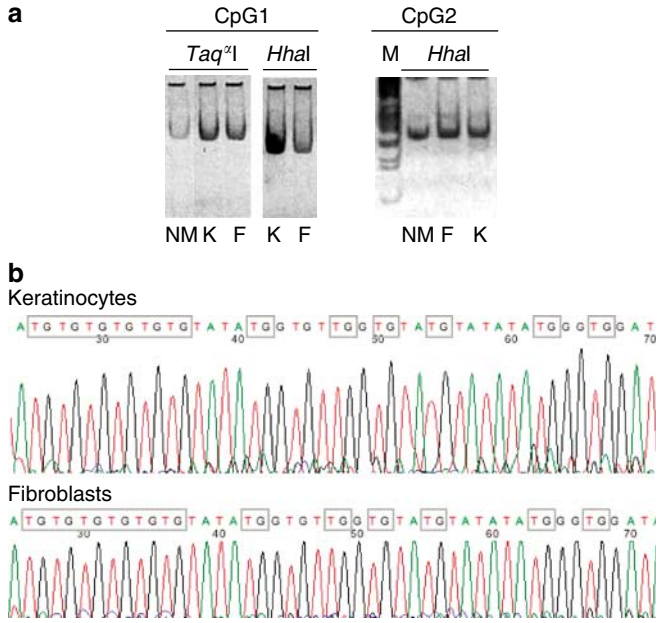

Figure 10. Cell-specific Rab33A suppression is not determined by promoter methylation. (**a**) COBRA analysis of CpG1 and CpG2 in keratinocytes (K) and fibroblasts (F) isolated from newborn foreskins, compared to normal melanocytes (NM). The figure shows reaction products of BS-modified DNA that had been amplified with BS1 and BS2 primers and digested with *Taq*$^{\alpha}$I or *Hha*I. (**b**) BS sequence analysis of CpG2. The results show that CpG2 amplified region in keratinocytes and fibroblasts that do not express Rab33A is unmethylated (gray boxes), in a fashion similar to that observed in YUOLD (Figure 8).

However, although CpG2 methylation was clearly associated with an inactive gene, the presence of the unmethylated allele was not sufficient to sustain Rab33A expression, because CpG2 was also not methylated in the non-expressing fibroblasts and keratinocytes. Interestingly, in whole skin, the Rab33A promoter was mostly methylated, suggesting differences between the stratified and proliferative epidermal layers. Cultured keratinocytes, such as those used in our experiments, are non-differentiated highly proliferating cells, whereas most of the keratinocytes in the skin are from the well-differentiated and stratified epidermal layer. Recent observations revealed differences in the expression of clusters of genes in native skin, cultured keratinocytes, and fibroblasts depending on the proliferative and differentiative state of these cells (Smiley *et al.*, 2005). Therefore, it is conceivable that some of these changes in gene expression may be the results of differences in DNA methylation.

Epigenetic modification is now widely recognized as one of the critical changes related to malignant transformation. Chromatin modification, in particular promoter methylation, is a highly valuable cancer biomarker because (a) DNA is stable, (b) the change is permanent, and (c) the procedure involves PCR amplification, and thus requires minute amounts of material, a limiting factor especially in the case of melanoma. In addition, the role of chromatin structure in carcinogenesis has made it a target for the treatment of malignancy (La Thangue, 2004; Mei *et al.*, 2004; Esteller, 2005a, b; Hess-Stumpp, 2005). Several tumor-related genes

are downregulated by promoter methylation in cancer cells, including melanoma. However, in most cases, the frequency of methylation varies, and no single gene so far has been identified as methylated in all melanoma tumors (Hoon *et al.*, 2004; van Doorn *et al.*, 2005). This situation may change, as more information from genome-wide studies will become available.

Abnormal expression of several X-linked genes has been documented in melanomas and other cancer cells. The best-known example is the MAGE gene family members located on Xq28 (Hoek *et al.*, 2004 and references within). We showed that *FGF13* that maps to chromosomal region Xq26.3, and is coordinately differentially expressed with MAGE genes in the different melanoma cell strains (Hoek *et al.*, 2004), suggesting aberrant activation of a potent growth factor by demethylation (Xiao *et al.*, 2005). It is thus possible that genes located on the X chromosome may be more susceptible to deregulation by epigenetic modification that can have an impact on malignant transformation and tumor progression.

MATERIALS AND METHODS

Cells and tissue samples

Normal cells. Normal human melanocytes, keratinocytes, fibroblasts, and endothelial cells were obtained from the Cell Culture Facility of the Yale Skin Disease Research Core Center (YSDRCC). Newborn melanocytes, keratinocytes, and fibroblasts were isolated from discarded foreskins. Adult melanocytes were isolated from the discarded skin obtained after voluntary abdominoplasty surgery of a 48-year-old female donor (AP48F). The human dermal microvascular endothelial cells were from normal adult single donor breast skin (passages 1 and 2) and were used for all experiments.

The normal human melanocytes were cultured in basal medium (Ham's F12 medium supplemented with 7% fetal calf serum and penicillin/streptocmycin) enriched with ingredients required for proliferation: TPA (50 nM, 12-*O*-tetradecanoyl phorbol-13-acetate), IBMX (0.1 mM, 3-isobutyl-1-methyl xanthin), Na_3VO_4 (1 μM), and dbcAMP (0.1 mM, N^6,2′-*O*-dibutyryladenosine 3:5-cyclic monophosphate), termed TICVA (Halaban, 2000). Keratinocytes were grown in KGM-2 medium (Clonetics, Division of BioWhittaker, Walkersville, MD) supplemented with calcium-depleted serum and the specific growth factors required for normal human keratinocytes supplied by Clonetics. Fibroblasts were cultured in the basal Ham's F12 medium, and endothelial cells in human dermal microvascular endothelial cell medium (EGM2-MV from BioWhittaker Cell Biology Products, Walkersville, MD), supplemented with 5% fetal calf serum plus a mixture of hydrocortisone, vascular endothelial growth factor, long recombinant 3-insulin-like growth factor-1, ascorbic acid, heparin, human recombinant epidermal growth factor, and gentamicin/amphotericin B.

Benign and malignant melanocytic lesions. We used a panel of cultured nevocytes, primary and metastatic melanoma cells, as well as snap-frozen and formalin-fixed paraffin-embedded tissues (Table 1). The study was conducted according to the Declaration of Helsinki Principles. Tissue samples were collected according to Health Insurance Portability and Accountability Act (HIPAA) regulations with Human Investigative Committee protocol. All lesional material was excised for the benefit of the patients, and only excess material was used without jeopardizing diagnosis or future treatment. Participants gave their written informed consent. The medical ethical committee of Yale University approved all described studies. The nevocytes from congenital giant nevi and a blue nevus and some of the primary melanoma cells (WW88 and WW94) were grown in the same growth factor-supplemented medium TICVA used for normal human melanocytes. The WW165 primary melanoma cells were grown with IBMX. The melanoma cells from metastatic lesions (YUMAC, YUDEW, and YUGUL) were grown in the basal Ham's F12 medium. Cells with the YU prefix, except for YUGEN8 and YUSIT1, were from short-term cultures (about 1 month) harvested during the first or second passage in culture. The melanoma cell strains 501 mel, 888 mel, 1241 mel, and 1335 mel were established in the Surgery Branch, National Cancer Institute, Bethesda, MD, and were maintained in OptiMEM medium supplemented with antibiotics and 7% fetal calf serum.

Rab33A peptide antiserum

Polyclonal antibodies to the peptide MAQPILGHGSLQPASAAGLA SLELDSSLDQYVQIR spanning the Rab33A N-terminus domain (synthesized by Yale Keck Foundation Biotechnology Laboratory, conjugated to KLH) were raised in rabbits by Cocalico Biological Inc., Reamstown, PA. Antiserum from one rabbit was determined to have a high titer when tested against a decreasing concentration of the peptide blotted on a polyvinyldine difluoride membrane (data not shown). The antiserum was partially purified with the Melon Gel Spin purification kit (Pierce, Rockford, IL) before use. This method was used because any attempts to purify the antibodies by immunoaffinity employing immobilized synthetic peptide or Protein A affinity column destroyed the specificity of the antibodies in response to low pH elution.

FlagRab33A constructs, transfection, expression, and subcellular localization

Rab33A (accession number NM_004794) was amplified from cDNA of normal human melanocytes employing 5′ oligonucleotide primers flanked with *Hin*dIII restriction site and the FLAG peptide TAAGCTTACC**ATGGACTACAAAGACGATGACGACAAG***GCGCAG CCCATCCTGGGC* (*Hin*dIII site underlined, the Flag encoding MDYKDDDDK in bold, and Rab33A sequences in italic) and 3′ oligonucleotide primers flanked with *Eco*RV digestion sites TTTTATTTTGATATC*AATTTGTATGGAAAC* (*Eco*RV site underlined, and Rab33A in italic), annealing temperature 55°C and subcloned into *Hin*dIII/*Eco*RV restriction sites of pcDNA 3.1. Rab33A-Q95L and Rab33A-T50N mutants were obtained by site-directed mutagenesis of the original FlagRab33A plasmid (QuikChange kit; Stratagene, La Jolla, CA). The fidelity of the constructs was verified by sequencing the inserts. Purified plasmid DNAs were then transfected into human melanoma cells (501 mel) employing the Lipofectamine 2000 reagent (Invitrogen Life Technologies, Carlsbad, CA) following the manufacturer's instructions. The expression of FlagRab33A protein was assessed by Western blotting 2 days post-transfection.

Western blotting

Cell pellets were washed in phosphate-buffered saline and lysed in RIPA buffer (PBS, 1% Nonidet P-40, 0.5% sodium deoxycholate, 0.1% SDS) supplemented with a cocktail of protease inhibitors

(''Complete'' Boehringer Mannheim Corp., Roche Molecular Biochemicals, Indianapolis, IN) with slight sonication. Total cell extracts (35 μg proteins/lane), measured by the Bio-Rad protein assay (Bio-Rad Laboratories, Hercules, CA), were prepared in samples buffer, heated to 95°C for 5 minutes, slightly sonicated for the second time, centrifuged to remove particulate material, fractionated in 8% polyacrylamide pre-cast gels (NuPAGE Bis-Tris, NOVEX, San Diego, CA), and transferred to a polyvinyldine difluoride membrane. The membrane was first probed with anti-Flag M2 mAb (Sigma-Aldrich, St Louis, MO) to detect ectopic protein followed by Rab33A polyclonal antibodies according to standard protocols. The expression level of endogenous protein was assessed by Western blot analysis of normal human melanocytes, melanoma cells, and freshly frozen melanoma tumor lysates with anti-Rab33A antibodies employing the same procedure.

Immunostaining

Cells. For subcellular localization, cells were grown on coverslips and processed for immunofluorescence analysis with anti-Flag (M2 mAb, Sigma-Aldrich), anti-Rab33A peptide antibodies, anti-Tyrp1 (mAb TA99) (Vijayasaradhi *et al*., 1991) or anti-gp100 (HMB45 mAb, DAKO Corporation, Carpinteria, CA) as described by Halaban *et al*. (2002). Coverslips were mounted with ProLong Gold anti-fade reagent with 4′,6-diamidino-2-phenylindole dihydrochloride (Molecular Probes, Invitrogen Corporation, Carlsbad, CA) to visualize nuclear DNA.

Mouse brain. All procedures involving animals were performed in strict accordance with the National Institutes of Health (NIH) Guidelines for the Care and Use of Laboratory Animals and were approved by the Yale Animal Care and Use Committee. Mice were anesthetized with chloral hydrate and perfused transcardially with 4% paraformaldehyde. Brains were dissected, post-fixed for 48 hours in 4% paraformaldehyde, cryoprotected in 30% sucrose, and cut into serial 35-μm parasagittal sections on a freezing microtome. Free floating sections were washed three times in potassium phosphate-buffered saline (KPBS), blocked in KPBS + 0.3% Triton X-100 + 4% normal serum, and incubated in anti-Rab33A antibodies at a 1:200 dilution overnight at 4°C. The following day, sections were washed three times in KPBS + 0.3% Triton X-100. After the washes, secondary antibodies (Alexa-568 anti-rabbit IgG; Molecular Probes, Eugene, OR) were added at a dilution of 1:2,000 for 1 hour at room temperature. The sections were washed three times in KPBS + 0.3% Triton X-100, twice in KPBS alone, and then incubated for 5 minutes in 0.7% Sudan Black B/70% methanol to quench autofluorescence. Sections were washed again and mounted onto positively charged slides in aqueous anti-fade mounting media (Biomeda, Foster City, CA). Photomicrographs were taken using a Zeiss Axioscope II microscope with ×63 objective. Images were processed using Adobe PhotoShop 7.0 (Adobe Systems, San Jose, CA) and Corel Draw 12.0 (Corel, Ottawa, ON, Canada). Images were adjusted for contrast and brightness to equilibrate light levels, and were cropped, resized, and rotated for purposes of presentation. In no case was the content of images altered.

Rab33A expression

High-quality total RNA was prepared from cell pellets with the TRIzol reagent (Invitrogen Life Technologies, Invitrogen Corporation, Carlsbad, CA). Poly(A) mRNA was isolated from total RNA employing the PolyATtract mRNA isolation system IV (Promega, Madison, WI) following the manufacturer's instructions. This additional step is required because melanin in total RNA suppresses PCR reactions. cDNA templates were generated from the Poly(A) selected RNAs using Invitrogen SuperScript II Reverse Transcriptase according to the manufacturer's instructions. The levels of Rab33A gene transcripts were assessed by RT-PCR employing the same primers used for cloning of Rab33A (see above, products size 835 bp), or with forward 5′-TCCCAGACAAGACTGAAGCCAC-3′ and backward 5′-GTTGCCCACAAGCACTTTGG-3′ primer pairs, annealing temperature 57.1°C, 35 cycles, product size 272 bp. As a control, expression of β-actin was assessed using forward 5′-GTGGG GCGCCCCAGGCACCA-3′ and backward primers 5′-CTCCTTAAT GTCACGGCACGATTTC-3′, annealing temperature 55°C, 35 cycles, product size 540 bp. All oligonucleotides were synthesized by the oligonucleotide synthesis facility at the Department of Pathology, Yale University School of Medicine.

DNA extraction

Cells and snap-frozen tissues. The DNeasy purification kit (Qiagen Inc., Valencia, CA) was used to extract the DNA from cell pellets and freshly frozen tumors.

Formalin-fixed paraffin-embedded material. The lesional sites in the formalin-fixed paraffin-embedded material were marked by a certified pathologist (J.M.), and 2 mm punch biopsy specimens were incubated in 300 μl DNA extraction buffer at 100°C for 1 hour to dissolve the paraffin. The samples were then digested with proteinase K overnight at 60°C, and DNA was purified by extraction with a phenol/chloroform solution. The quality of the DNA was analyzed by gel fractionation and UV light visualization.

Analyses of *Rab33A* proximal promoter methylation

Primer design (Table 2) was based on human DNA sequence from clone RP3-438D16 on chromosome Xq24–26.1 (Accession no. AL139234) employing the web-based MethPrimer program for designing BS conversion-based Methylation PCR Primers (Li and Dahiya, 2002) at http://www.urogene.org/methprimer/index1.html. Primers that amplify the unmodified promoter region were used to demonstrate that this region is intact in various melanoma cell strains and tumors. All methylation analyses were performed on samples that originated from male individuals in order to avoid contribution from the female X-inactivated chromosome.

Genomic DNA was isolated and a total of 2 μg was modified by sodium BS. Reactions were hot started at 94°C for 5 minutes after which 1 U of Platinum *Taq* polymerase (Invitrogen Life Technologies, Invitrogen Corporation, Carlsbad, CA) was added followed by 35–40 cycles of 94°C for 30 seconds, optimal annealing temperature (Table 2) for 30 seconds, extension at 72°C for 30 seconds, and finally 5 minutes at 72°C. PCR reaction products were loaded onto 1% agarose gel, stained with ethidium bromide, and visualized under UV illumination.

For COBRA analysis, the DNA was amplified with primers that bind to the BS-treated DNA in non-CpG regions in the converted DNA (Table 2), and the amplified products (35–40 cycles) were gel purified. The restriction enzymes used for further analyses were *Hha*I, *Taq*$^{\alpha}$1, *Bsi*E1, *Nco*I (New England Biolabs, Hanover, MD) and

Table 2. Oligonucleotide primers for amplification of Rab33A promoter

Application	Relative to TS	Designation	Primers	T_{an} (°C)	Product size (nt)
PCR wt	−231 to −208	WTF	5′-GGCAAGGAGAAAGAAGTCTATCCC-3′	61.4	265
	+33 to +14	WTB	5′-CGGAGGCACCAACACAAAAG-3′		
CpG island 1					
COBRA	−233 to −209	BS1F	5′-GGGGTAAGGAGAAAGAAGTTTATTT-3′	52.9	263
	+29 to +4	BS1B	5′-AACACCAACACAAAAACCAAAA-3′		
Nested for BS sequencing		BS1Ba	5′-CCAAAAAAAAAAAAAAAAAAAAAAAAAAAT-3′		247
MSP1 nested	−232 to −208	M1F	F: 5′- GGGTAAGGAGAAAGAAGTTTATTTC -3′	53.3	182
	−51 to −72	M1B	B: 5′-TCGAACCGAATACTCTAACGAA-3′		
	−233 to −216	U1F	F: 5′-GGGGTAAGGAGAAAGAAGTTTATTT-3′	51.8	186
	−48 to −82	U1B	B: 5′-CCCTCAAACCAAATACTCTAACAAA -3′		
CpG island 2					
BS2	+75 to +96	BS2F	5′-GGAGTGAGAGGTATTTTTTTTA-3′	51.9	226
	+300 to +270	BS2B	5′-ACTACAAACTCCCATAACCCAAA-3′		
MSP2	+152 to +179	M2F	5′-CGCGCGTATATATATACGTATAGAGTTC-3′	53.3	205
	+356 to +335	M2B	5′-GTACTAATCCAACGACGAATCG-3′		
	+151 to +180	U2F	5′-ATGTGTGTATATATATATGTATAGAGTTTG-3′	55.4	211
	+361 to +335	U2B	5′-TACACATACTAATCCAACAACAAATCA-3′		
CpG island 3					
BS3	+274 to +298	BS3F	5′-TTATTTTGGGTTATGGGAGTTTGTA-3′	52.1	264
BS3	+538 to +513	BS3B	5′-TAACCCCCTAAATCACCTTAATCTT-3′		

TS, transcription start site; T_{an}, annealing temperature; nt, nucleotides; wt, wild-type non-modified DNA; BS, bisulfite.
BS primers bind to modified DNA avoiding CpG dinucleotides. M and U primers, respectively, bind preferentially to unmethylated and methylated DNA BS-modified and -amplified DNA: F and B, forward and backward primers, respectively. See Figure 4a for schematic representation of primer locations.

*Mae*II (Roche Molecular Biochemicals, Indianapolis, IN), which cut unconverted (methylated) but not converted (unmethylated) DNA. Digestion was stopped with 1 μl of 1% SDS for 10 minutes at 65°C, to prevent band-shift in polyacrylamide gel owing to binding of protein to DNA. For BS-MSP, the amplified region was subjected to a second PCR amplification with internal primers that are methylation specific (Table 2). For MSP analysis, PCR amplification was performed directly with primers that selectively bind to converted (unmethylated) or non-converted (methylated) sequences. For BS-sequencing analysis, PCR was performed using the same BS primers described above for COBRA (Table 2), PCR products were gel purified and the fragments were sequenced by Applied Biosystems 3730 capillary instruments at the W.M. Keck Foundation Biotechnology Resource Laboratory at Yale, employing fluorescence-labeled dideoxynucleotides.

MSP and BS-MSP products were loaded onto 1% agarose gels, stained with ethidium bromide, and visualized under UV illumination. In most cases, COBRA amplification products were fractionated in non-denaturing 8% polyacrylamide gels, stained with ethidium bromide, and visualized under UV illumination.

Effects of 5-Aza-CdR on gene regulation and DNA methylation
5-Aza-CdR (Sigma Chemical Co., St Louis, MO) was dissolved in methanol as 10 mM stock solution, aliquoted, and kept at −20°C. Sparse cultures of proliferating melanoma cells were grown in regular Ham's F10 medium (control) or in medium supplemented with 0.1 or 0.2 μM final concentration of 5-Aza-CdR for 2 days, with fresh drug-containing medium being added on the second day. This concentration was chosen to avoid cytotoxicity because dose-response analyses employing several melanoma cell strains showed that melanoma cells are highly sensitive and stop proliferating when incubated with 0.5 μM or higher concentrations of 5-Aza-CdR (data not shown). The cells were then released into regular medium, allowed to recover for additional 2 days, harvested, and the levels of Rab33A gene transcripts were assessed by RT-PCR employing Rab33A-specific primer set 2 (Table 2). In addition, genomic DNA was collected to identify changes in Rab33A promoter methylation in response to 5-Aza-CdR.

CONFLICT OF INTEREST
The authors state no conflict of interest.

ACKNOWLEDGMENTS
We thank Donna LaCivita (Department of Dermatology) and Aaron J. Berger (Department of Pathology) for technical assistance, Drs Barry Richter and Rossitza Lazova for providing nevus specimens, and Dr Lisa Brailey for editorial assistance. This work was supported by NIH/NCI Grant 1 R21 CA 113741 and Yale Cancer Center Translational Research Awards in Cancer to R.H., and NIAMS Grant AR041942 (Dr Robert Tigelaar PI), R21AR051723 (Dr Sherman Weissman, PI), and NIH Grant 5R01CA115756-02 to H.M.K. Dr Daniela Kovacs was supported by funding from the US–Italian project (Progetto Italia–USA Grant 530/F-A1).

SUPPLEMENTARY MATERIAL
Figure S1. CpG1 BS-sequence analysis.

REFERENCES

Ballestar E, Esteller M (2005a) The epigenetic breakdown of cancer cells: from DNA methylation to histone modifications. *Prog Mol Subcell Biol* 38:169–81

Ballestar E, Esteller M (2005b) Methyl-CpG-binding proteins in cancer: blaming the DNA methylation messenger. *Biochem Cell Biol* 83: 374–84

Berrettini WH (2000) Genetics of psychiatric disease. *Annu Rev Med* 51:465–79

Bird A (2002) DNA methylation patterns and epigenetic memory. *Genes Dev* 16:6–21

Chen WY, Baylin SB (2005) Inactivation of tumor suppressor genes: choice between genetic and epigenetic routes. *Cell Cycle* 4:10–2

Cheng KW, Lahad JP, Gray JW, Mills GB (2005) Emerging role of RAB GTPases in cancer and human disease. *Cancer Res* 65:2516–9

Cheng KW, Lahad JP, Kuo WL, Lapuk A, Yamada K, Auersperg N *et al.* (2004) The RAB25 small GTPase determines aggressiveness of ovarian and breast cancers. *Nat Med* 10:1251–6

Costello JF, Plass C (2001) Methylation matters. *J Med Genet* 38:285–303

D'Adamo P, Menegon A, Lo Nigro C, Grasso M, Gulisano M, Tamanini F *et al.* (1998) Mutations in GDI1 are responsible for X-linked non-specific mental retardation. *Nat Genet* 19:134–9

Deneka M, Neeft M, van der Sluijs P (2003) Regulation of membrane transport by rab GTPases. *Crit Rev Biochem Mol Biol* 38:121–42

Di Pietro SM, Dell'Angelica EC (2005) The cell biology of Hermansky–Pudlak syndrome: recent advances. *Traffic* 6:525–33

Esteller M (2005a) Aberrant DNA methylation as a cancer-inducing mechanism. *Annu Rev Pharmacol Toxicol* 45:629–56

Esteller M (2005b) DNA methylation and cancer therapy: new developments and expectations. *Curr Opin Oncol* 17:55–60

Esteller M, Gaidano G, Goodman SN, Zagonel V, Capello D, Botto B *et al.* (2002) Hypermethylation of the DNA repair gene O(6)-methylguanine DNA methyltransferase and survival of patients with diffuse large B-cell lymphoma. *J Natl Cancer Inst* 94:26–32

Esteller M, Hamilton SR, Burger PC, Baylin SB, Herman JG (1999) Inactivation of the DNA repair gene O6-methylguanine-DNA methyltransferase by promoter hypermethylation is a common event in primary human neoplasia. *Cancer Res* 59:793–7

Esteller M, Risques RA, Toyota M, Capella G, Moreno V, Peinado MA *et al.* (2001) Promoter hypermethylation of the DNA repair gene O(6)-methylguanine-DNA methyltransferase is associated with the presence of G:C to A:T transition mutations in p53 in human colorectal tumorigenesis. *Cancer Res* 61:4689–92

Evans TM, Simpson F, Parton RG, Wicking C (2005) Characterization of Rab23, a negative regulator of sonic hedgehog signaling. *Methods Enzymol* 403:759–77

Feig LA (1999) Tools of the trade: use of dominant-inhibitory mutants of Ras-family GTPases. *Nat Cell Biol* 1:E25–7

Feinberg AP, Tycko B (2004) The history of cancer epigenetics. *Nat Rev Cancer* 4:143–53

Frommer M, McDonald LE, Millar DS, Collis CM, Watt F, Grigg GW *et al.* (1992) A genomic sequencing protocol that yields a positive display of 5-methylcytosine residues in individual DNA strands. *Proc Natl Acad Sci USA* 89:1827–31

Guo A, Wang T, Ng EL, Aulia S, Chong KH, Teng FY *et al.* (2006) Open brain gene product Rab23: expression pattern in the adult mouse brain and functional characterization. *J Neurosci Res* 83:1118–27

Halaban R (2000) The regulation of normal melanocyte proliferation. *Pigment Cell Res* 13:4–14

Halaban R, Cheng E, Svedine S, Aron R, Hebert DN (2001) Proper folding and ER to Golgi transport of tyrosinase are induced by its substrates, DOPA and tyrosine. *J Biol Chem* 276:11933–8

Halaban R, Patton RS, Cheng E, Svedine S, Trombetta ES, Wahl ML *et al.* (2002) Abnormal acidification of melanoma cells induces tyrosinase retention in the early secretory pathway. *J Biol Chem* 277:14821–8

Halaban R, Svedine S, Cheng E, Smicun Y, Aron R, Hebert DN (2000) Endoplasmic reticulum retention is a common defect associated with tyrosinase-negative albinism. *Proc Natl Acad Sci USA* 97:5889–94

Herman JG, Graff JR, Myohanen S, Nelkin BD, Baylin SB (1996) Methylation-specific PCR: a novel PCR assay for methylation status of CpG islands. *Proc Natl Acad Sci USA* 93:9821–6

Hess-Stumpp H (2005) Histone deacetylase inhibitors and cancer: from cell biology to the clinic. *Eur J Cell Biol* 84:109–21

Hoek K, Rimm DL, Williams KR, Zhao H, Ariyan S, Lin A *et al.* (2004) Expression profiling reveals novel pathways in the transformation of melanocytes to melanomas. *Cancer Res* 64:5270–82

Hoon DS, Spugnardi M, Kuo C, Huang SK, Morton DL, Taback B (2004) Profiling epigenetic inactivation of tumor suppressor genes in tumors and plasma from cutaneous melanoma patients. *Oncogene* 23:4014–22

Jacobsen M, Repsilber D, Gutschmidt A, Neher A, Feldmann K, Mollenkopf HJ *et al.* (2005) Ras-associated small GTPase 33A, a novel T cell factor, is down-regulated in patients with tuberculosis. *J Infect Dis* 192:1211–8

Jaenisch R, Bird A (2003) Epigenetic regulation of gene expression: how the genome integrates intrinsic and environmental signals. *Nat Genet* 33:245–54

Klose RJ, Bird AP (2006) Genomic DNA methylation: the mark and its mediators. *Trends Biochem Sci* 31:89–97

Kutsche K, Yntema H, Brandt A, Jantke I, Nothwang HG, Orth U *et al.* (2000) Mutations in ARHGEF6, encoding a guanine nucleotide exchange factor for Rho GTPases, in patients with X-linked mental retardation. *Nat Genet* 26:247–50

La Thangue NB (2004) Histone deacetylase inhibitors and cancer therapy. *J Chemother* 16(Suppl 4):64–7

Li LC, Dahiya R (2002) MethPrimer: designing primers for methylation PCRs. *Bioinformatics* 18:1427–31

Mei S, Ho AD, Mahlknecht U (2004) Role of histone deacetylase inhibitors in the treatment of cancer (review). *Int J Oncol* 25:1509–19

Novick P, Zerial M (1997) The diversity of Rab proteins in vesicle transport. *Curr Opin Cell Biol* 9:496–504

Osanai K, Takahashi K, Nakamura K, Takahashi M, Ishigaki M, Sakuma T *et al.* (2005) Expression and characterization of Rab38, a new member of the Rab small G protein family. *Biol Chem* 386:143–53

Paulsen M, Ferguson-Smith AC (2001) DNA methylation in genomic imprinting, development, and disease. *J Pathol* 195:97–110

Raymond FL (2005) X-linked mental retardation: a clinical guide. *J Med Genet* 43:193–200

Sasaki M, Anast J, Bassett W, Kawakami T, Sakuragi N, Dahiya R (2003) Bisulfite conversion-specific and methylation-specific PCR: a sensitive technique for accurate evaluation of CpG methylation. *Biochem Biophys Res Commun* 309:305–9

Seabra MC, Coudrier E (2004) Rab GTPases and myosin motors in organelle motility. *Traffic* 5:393–9

Smiley AK, Klingenberg JM, Aronow BJ, Boyce ST, Kitzmiller WJ, Supp DM (2005) Microarray analysis of gene expression in cultured skin substitutes compared with native human skin. *J Invest Dermatol* 125:1286–301

Stein MP, Dong J, Wandinger-Ness A (2003) Rab proteins and endocytic trafficking: potential targets for therapeutic intervention. *Adv Drug Deliv Rev* 55:1421–37

Stenmark H, Olkkonen VM (2001) The Rab GTPase family. *Genome Biol* 2 REVIEWS3007.1-3007.7

Su AI, Wiltshire T, Batalov S, Lapp H, Ching KA, Block D *et al.* (2004) A gene atlas of the mouse and human protein-encoding transcriptomes. *Proc Natl Acad Sci USA* 101:6062–7

van Doorn R, Zoutman WH, Dijkman R, de Menezes RX, Commandeur S, Mulder AA *et al.* (2005) Epigenetic profiling of cutaneous T-cell

lymphoma: promoter hypermethylation of multiple tumor suppressor genes including BCL7a, PTPRG, and p73. *J Clin Oncol* 23:3886–96

Vijayasaradhi S, Doskoch PM, Houghton AN (1991) Biosynthesis and intracellular movement of the melanosomal membrane glycoprotein gp75, the human b (brown) locus product. *Exp Cell Res* 196:233–40

Vijayasaradhi S, Xu YQ, Bouchard B, Houghton AN (1995) Intracellular sorting and targeting of melanosomal membrane proteins – identification of signals for sorting of the human brown locus protein, gp75. *J Cell Biol* 130:807–20

Xiao J, Chen HS, Fei R, Cong X, Wang LP, Wang Y *et al.* (2005) Expression of MAGE-A1 mRNA is associated with gene hypomethylation in hepatocarcinoma cell lines. *J Gastroenterol* 40:716–21

Zheng JY, Koda T, Arimura Y, Kishi M, Kakinuma M (1997) Structure and expression of the mouse S10 gene. *Biochim Biophys Acta* 1351:47–50

Zheng JY, Koda T, Fujiwara T, Kishi M, Ikehara Y, Kakinuma M (1998) A novel Rab GTPase, Rab33B, is ubiquitously expressed and localized to the medial Golgi cisternae. *J Cell Sci* 111(Part 8):1061–9